Discovery of a Rhodanine Class of Compounds as Inhibitors of *Plasmodium falciparum* Enoyl-Acyl Carrier Protein Reductase

Gyanendra Kumar,[†] Prasanna Parasuraman,[†] Shailendra Kumar Sharma,[†] Tanushree Banerjee,[‡] Krishanpal Karmodiya,[§] Namita Surolia,[§] and Avadhesha Surolia*,[†,‡]

Molecular Biophysics Unit, Indian Institute of Science, Bangalore 560012, India, National Institute of Immunology, New Delhi 110067, India, and Molecular Biology and Genetics Unit, Jawaharlal Nehru Centre for Advanced Scientific Research, Bangalore, 560064, India

Enoyl acyl carrier protein (ACP) reductase, one of the enzymes of the type II fatty acid biosynthesis pathway, has been established as a promising target for the development of new drugs for malaria. Here we present the discovery of a rhodanine (2-thioxothiazolidin-4-one) class of compounds as inhibitors of this enzyme using a combined approach of rational selection of compounds for screening, analogue search, docking studies, and lead optimization. The most potent inhibitor exhibits an IC_{50} of 35.6 nM against *Plasmodium falciparum* enoyl ACP reductase (PfENR) and inhibits growth of the parasite in red blood cell cultures at an IC_{50} value of 750 nM. Many more compounds of this class were found to inhibit PfENR at low nanomolar to low micromolar concentrations, expanding the scope for developing new antimalarial drugs. The structure−activity relationship of these rhodanine compounds is discussed.

Introduction

Over three billion people live under the threat of malaria across the world and it kills over a million each year, mostly children.[1] Of the four species of *Plasmodium* that cause human malaria, *Plasmodium falciparum* accounts for the most severe and fatal form of the disease, cerebral malaria. Malaria has primarily been treated with chloroquine or pyrimethamine-sulfadoxine. Emergence of strains of the pathogen resistant to these drugs has made the situation worse.[2] Hence, finding novel pathways unique to the malaria parasite and identifying lead compounds against these pathways becomes necessary. Our recent discovery of a type II fatty acid synthesis pathway in *Plasmodium* has opened new avenues for drug development against malaria.[3]

Type II fatty acid synthase (FAS[a] II), present in prokaryotes, plants, and some protozoans, is structurally different from FAS-I (fatty acid synthase I) found in the human host as well as other higher eukaryotes, yeast, and certain mycobacteria. While FAS-II has discrete enzymes catalyzing individual reactions of the pathway,[4] FAS-I consists of a single multifunctional protein in which various domains catalyze different reactions of the biosynthetic pathway.[5]

In *P. falciparum*, type II fatty acid synthesis has been localized in the relict plastid called apicoplast, which is evolutionarily related to cyanobacteria.[6] The striking difference in the organization of the FAS catalyzing fatty acid synthesis in *P. falciparum* and *Escherichia coli* with that in the human host makes this pathway a potent drug target not only for developing drugs against *Plasmodium*, but also against a number of other infectious organisms harboring type II FAS.

The elongation module of fatty acid biosynthesis consists of four iterative steps: decarboxylative condensation, NADPH-

Scheme 1. Enoyl-ACP Reductase Catalyzed Reaction, Which Reduces the *trans*-Double Bond between C_2 and C_3 of the Growing Fatty Acyl Chain Using NADH
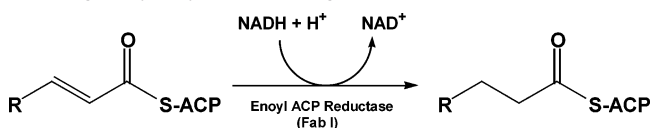
dependent reduction, dehydration, and NADH-dependent reduction.[4,5] The fourth step of NADH-dependent reduction is carried out by enoyl-acyl carrier protein (ACP) reductase (ENR), which reduces the trans-2 enoyl bond of enoyl-ACP substrates to saturated acyl-ACPs. This step has been shown to be a rate determining step in *E. coli* fatty acid biosynthesis (Scheme 1),[7] which makes it an ideal point of intervention therapeutically. It has been validated as a potential antimalarial[3,8] and antibacterial[9] drug target. The suitability of ENR as a drug target has been discussed in detail previously.[9,10] Extensive studies have been done by us on *P. falciparum* ENR (PfENR) using biochemical[11−14] as well as structural[15−17] tools to understand the mechanism of its inhibition by triclosan. Triclosan was found effective in killing *P. falciparum* in vitro and was able to cure mice of infection with the rodent malaria species *P. berghei* as well as acute bacterial infection.[3,18] Recently, a number of analogs of triclosan were designed and tested by us and others against PfENR.[19−21] Though the study of the structure−activity relationship of triclosan and its analogs provided good insight into the roles of various functional groups, none of the compounds showed significantly better activity over triclosan. We also synthesized and tested some substituted pyrazoles, which exhibited moderate inhibitory activity against PfENR.[22] Recently, we have reported that green tea catechins are potent inhibitors of PfENR and we have also reported their potentiation of the inhibitory activity of triclosan for PfENR.[23]

To expand the range of available pharmacophores from which new ENR inhibitors can be developed, we have tested a diverse set of compounds selected from Chemical Diversity Labs against PfENR. Here we report the identification and evaluation of a novel class of compounds with different core moieties that inhibit PfENR. The most effective compounds contained a

---

* To whom correspondence should be addressed. A. Surolia, National Institute of Immunology, Aruna Asaf Ali Marg, New Delhi 110067, India. Tel.: 91-11-26717102. Fax: 91-11-26717104. E-mail: surolia@nii.res.in.
† Indian Institute of Science.
‡ National Institute of Immunology.
§ Jawaharlal Nehru Centre for Advanced Scientific Research.
a Abbreviations: FAS, fatty acid synthase; ACP, acyl carrier protein; PfENR, *Plasmodium falciparum* enoyl-ACP reductase; Pf; *Plasmodium falciparum*; Ec, *Escherichia coli*; K_i, dissociation constant; TCL, triclosan.
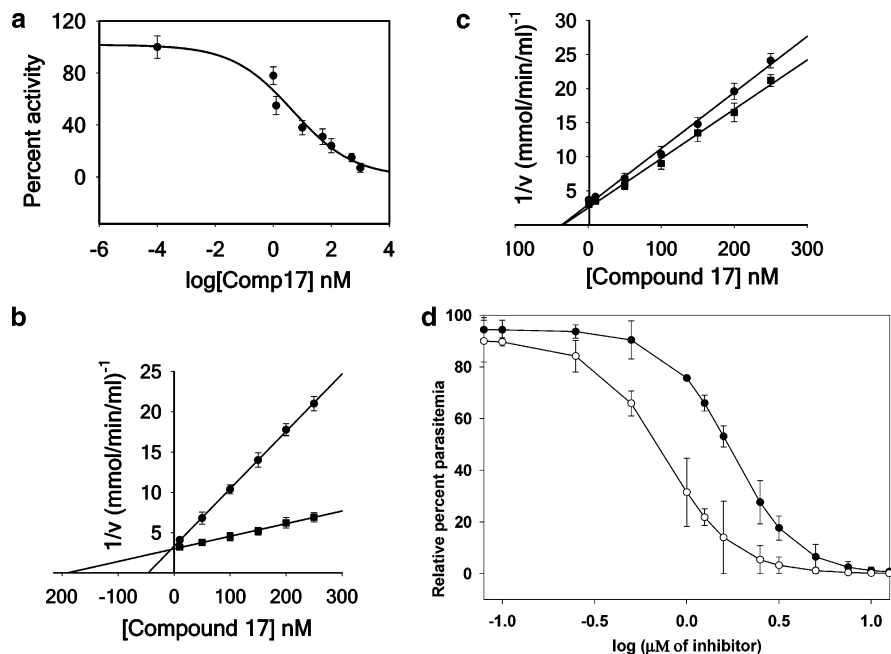
Figure 1. (a) Inhibition of PfENR by compound **17**. PfENR activity was determined in the presence of various concentrations of the inhibitor (25−750 nM). The percent inhibition was calculated from the residual PfENR activity and was plotted against log [compound **17**] used. The sigmoidal curve indicates the best fit for the data, and the IC_{50} value was calculated from the graph. Each point in the graph is the mean value calculated from three different sets of experiments, and the error bars show the standard deviation of the data. (b) Inhibition kinetics of compound **17** with respect to crotonoyl CoA were determined using the Dixon plot. PfENR was assayed at two fixed concentrations, 100 μM [●] and 200 μM [■], of crotonoyl CoA in presence of 250 nM of compound **17** and 100 μM of NADH. K_i was calculated from the x-intercept. The plot indicates competitive kinetics with respect to crotonoyl CoA. Each point in the graph represents the mean value calculated from three different sets of experiments, and the error bars show the standard deviation of the data. (c) Inhibition kinetics of compound **17** with respect to NADH were determined using the Dixon plot. PfENR (200 nM) was assayed in the presence of 200 μM of crotonoyl CoA, 250 nM of compound **17**, and 50 μM [●] and 100 μM [■] of NADH. K_i of inhibitor was calculated from the x-intercept. The plot indicates noncompetitive kinetics with respect to NADH. The data points of the plots are the mean value of three different sets of experiments, and the error bars show the standard deviation of the data. (d) Inhibition of growth of the parasite in red blood cell cultures. Compound **17** was assayed for in vitro growth inhibition of *P. falciparum* by incubating the cultures with different concentrations of the inhibitors in Me$_2$SO (final concentration, 0.05%). The cultures were checked for growth inhibition by microscopic examination by assessing the parasitemia at every 48 h (●) and 96 h (○). Each data point represents the mean value calculated from three different set of experiments, and the error bars show the standard deviation of the data.

common core commonly known as rhodanines. This class of small molecule inhibitors has been previously known to possess pharmacological activities against various biological targets ranging from aldose reductase,[24] β-lactamase,[25] HCV NS3 protease,[26] UDP−N-acetylmuramate/L-alanine ligase,[27] cathepsin,[28] and histidine decarboxylase[29] and is also shown to have antidiabetic activity.[21] In the present work, for the first time we report a rhodanine class of compounds as novel and potent inhibitors of ENR from *Plasmodium falciparum*. Further, the mechanisms of inhibition of PfENR by these compounds along with their structure−activity relationship was probed, which provide insights for further optimization of lead compounds of this class and generation of a pharmacophore model.

Results and Discussion

ENR has been well established as a potent target for designing antibacterials as well as antimalarials.[3,16] The frontline drug against tuberculosis, isoniazid, also targets ENR of *Mycobacterium tuberculosis*.[30] Availability of atomic structures of ENR from *P. falciparum* and other pathogenic organisms like *E. coli* make it possible to attempt structure-based drug design against malaria as well as bacterial diseases. Atomic structures of ENR−NAD$^+$−triclosan complex and that of ENR−NAD$^+$ with other inhibitors like diazoborines, imidazoles, and aminopyridines provide insights on the key features of ENR inhibition.[31−33] The two most striking features are (1) at least one of the rings in the inhibitors participate in π-stacking interactions with the

nicotinamide ring of the cofactor NADH and (2) the inhibitor forms a hydrogen bond with the active site residue, tyrosine. In the case of PfENR−NAD$^+$−triclosan ternary complex, ring A of triclosan nestles in a hydrophobic pocket made up of residues Tyr^{267}, Tyr^{277}, Gly^{313}, Pro^{314}, Ile^{323}, Phe^{368}, Ile^{369}, and Ala^{372}. The ring A stacks with the nicotinamide moiety of the oxidized cofactor NAD$^+$ (Figure 2a). Also, five hydrogen bonds between NAD$^+$ and the substrate-binding loop of PfENR stabilize the ternary complex of the enzyme with NAD$^+$ and triclosan.

To identify new lead compounds against PfENR, we took the above key features of interactions between the enzyme and the inhibitor as well as those between NAD$^+$ and inhibitor into consideration and selected 382 compounds representing a diverse set of scaffolds from a database of ~200 000 compounds (Chemical Diversity Labs, Moscow; Chart 1). These 382 representative compounds were tested for their inhibitory activity against purified PfENR in a spectrophotometric assay. Thirty-one compounds among them were found to be active against PfENR at ≤100 μM, the best four of which showed IC_{50} values of 6.0, 6.5, 7.0, and 10 μM. These four compounds had a common core moiety, that is, 2-thioxothiazolidin-4-one. Such compounds are commonly known as rhodanines. We took all the analogues of these four compounds from the database and conducted docking studies on them using AutoDock to calculate their binding energies against PfENR and selected 32 additional compounds with better binding energies compared to the four hits found earlier. We tested these compounds for their inhibitory
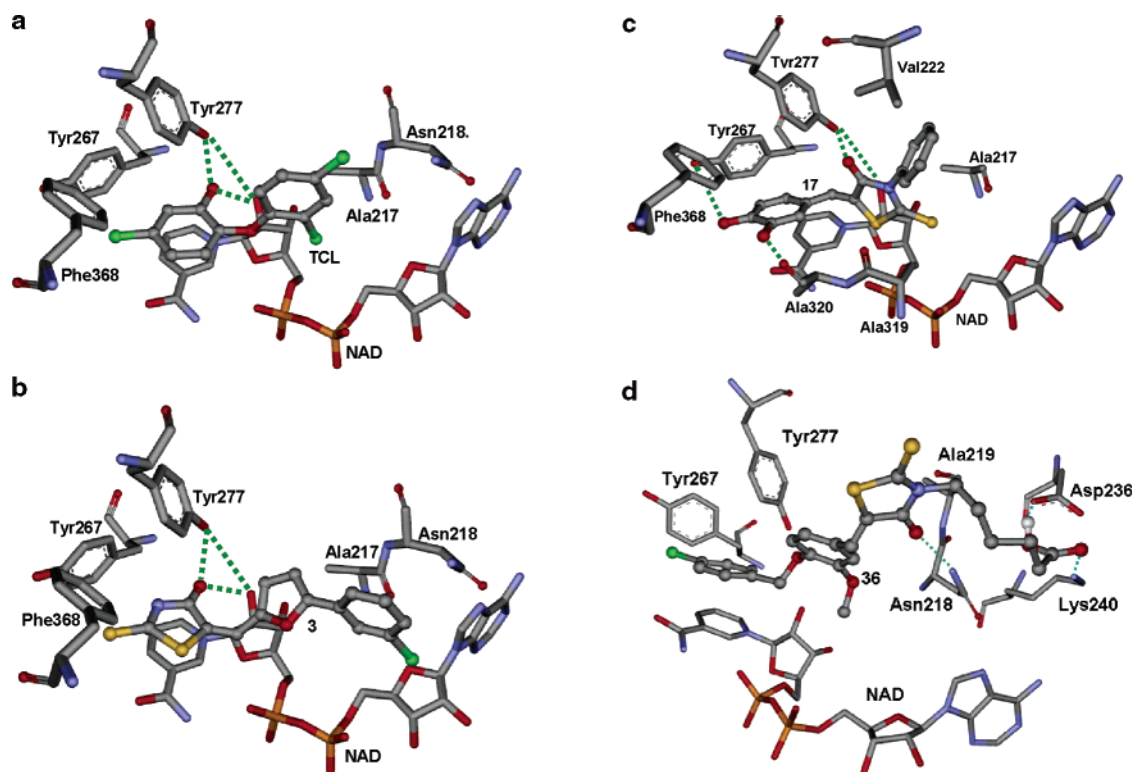
Figure 2. (a) Interactions of triclosan in the cocrystallized ternary complex PfENR and NAD. Triclosan is shown in ball and sticks and NAD and amino acids are shown in sticks. Atoms are colored in their elemental color format: carbon, gray; oxygen, red; nitrogen, blue; chlorine, green; phosphorus, orange. Hydrogen bonds are shown with green dotted lines. (b) Interactions of compound **1** with PfENR and NAD, as deduced by docking. Color-coding and cartoon representation is as described in Figure 2a. (c) Interactions of compound **17** with PfENR and NAD, as deduced by docking. Color-coding and cartoon representation is as described in Figure 2a. (d) Interactions of compound **36** with PfENR and NAD, as deduced by docking. Color-coding and cartoon representation is as described in Figure 2a.

activity against PfENR and found that nine of them possess the activity (Scheme 2). The best compound among them (compound **17**) gave an IC_{50} of 35.6 nM. The most active compounds belong to two related classes of compounds (Tables 1, 2 and 3), but sharing a common core moiety, that is, 2-thioxo-thiazolidin-4-one, commonly known as rhodanine. One class of these rhodanines has a furan ring attached to the 2-thioxo-thiazolidin-4-one core moiety through a methylene linker, while the other class has a benzene ring attached to the 2-thioxo-thiazolidin-4-one core moiety in a similar way. Other than rhodanines, we identified four compounds having quinoline/quinazoline scaffold as the core moiety, with IC_{50} values from 50 to 60 μM. Also a few individual molecules belonging to different classes of compounds showed moderate inhibitory activities against PfENR. Triclosan was used as a positive control and it exhibited an IC_{50} of 66 nM and K_i of 53 nM. So, the most potent rhodanine compound (**17**) is better as an inhibitor compared to triclosan.
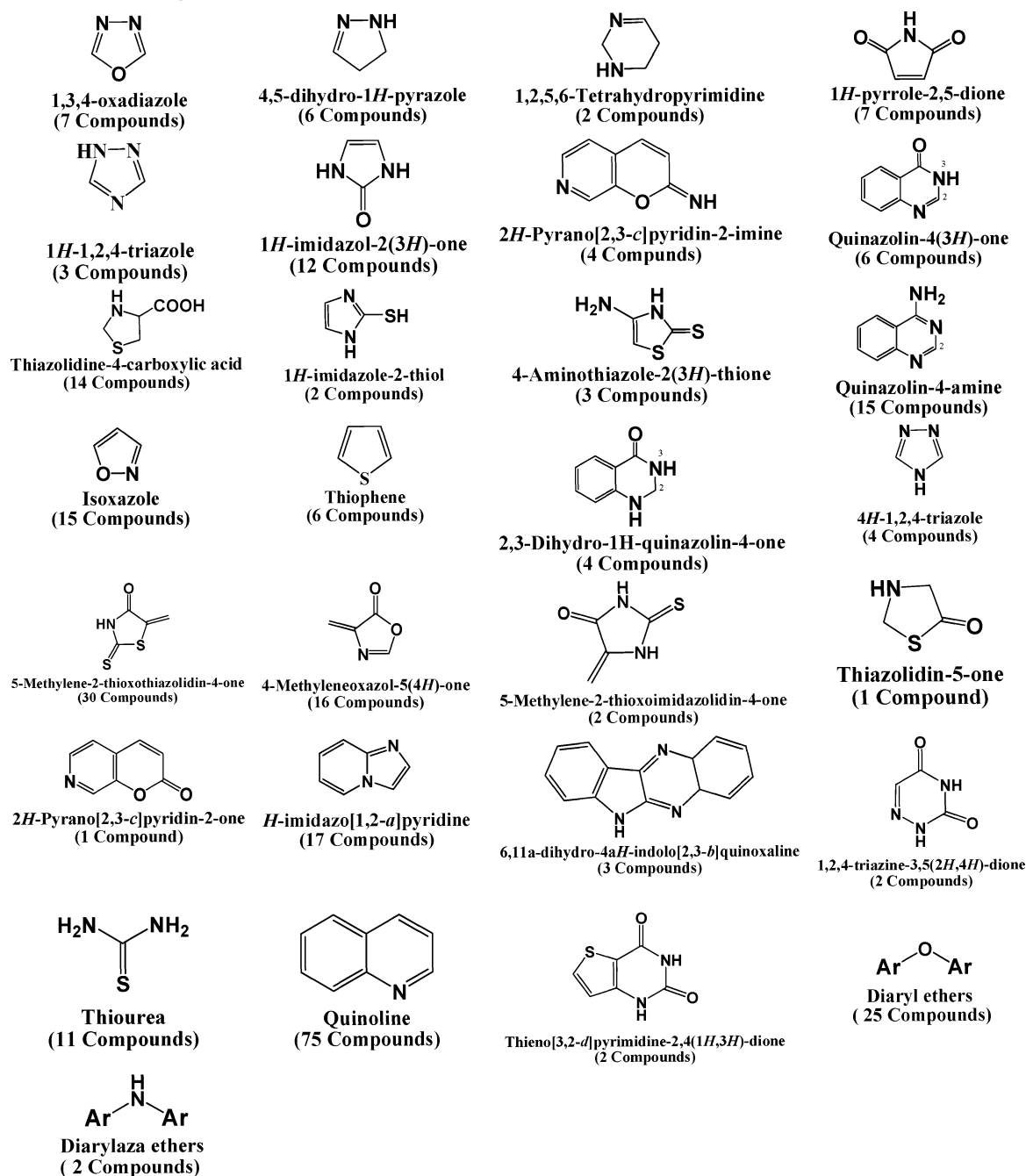
Rhodanine derivatives are known to possess biological activities as anticonvulsant, antibacterial, antiviral, and antidiabetic.[34,35] They have been found to inhibit some other targets previously, for example, arylalkylidene rhodanines with bulky and hydrophobic functional groups were found to inhibit hepatitis C virus (HCV) nonstructural protein 3 (NS3), a serine protease with IC_{50} values in low micromolar range,[26] rhodanine-3-acetic acid derivatives have been found to inhibit *Candida albicans* protein mannosyl transferase 1 (PMT1) with IC_{50} values in 0.2−0.5 μM range,[36] some rhodanine derivatives have been found to inhibit the phosphatase of regenerating liver (PRL) family tyrosine phosphatase 3 (PRL-3) at an IC_{50} value of 0.9 μM.[37] Other rhodanines have been found to inhibit JNK-stimulating phosphatase-1 (JSP-1) in low micromolar range

(1.2−20 μM)[38] and to inhibit Anthrax lethal factor protease in micromolar to submicromolar range.[39,40] A rhodanine derivative has been recently found to prevent biofilm formation by *Staphylococcus epidermidis*.[41] In a recent screening, some rhodanine derivatives have emerged as inhibitors of the enzymes involved in the synthesis of L-rhamnosyl residue (IC_{50} = 10μM), a part of *Mycobacterium tuberculosis* cell wall.[42] The rhodanine derivatives described in this manuscript display inhibitory activity against PfENR which are better than that against any other targets explored so far, and hence, they make potential lead compounds for further exploration as antimalarial agents. The kinetic data are shown for compound **17** as a representative example among the rhodanines tested.

Kinetics of the Inhibition of PfENR by Rhodanines. PfNER was expressed, purified, and its activity was checked as described earlier.[11,12] The IC_{50} values for the 10 best inhibitors were determined as described in the Experimental Section. Five of these are rhodanines with furan moiety attached through a methylene linker, and the other five are rhodanines with phenyl moiety attached through a methylene linker. The residual PfENR activity was plotted against the log of the respective inhibitor concentration using a nonlinear regression method. The best fit of the data gave a sigmoidal curve from which IC_{50} values were calculated (Figure 1a). The IC_{50} value for the best compound, compound **17**, was found to be 35.6 nM.

We then deduced the mechanisms of inhibition for each of the ten inhibitors with respect to substrate analog crotonoyl-CoA as well as the cofactor, NADH. All the inhibition data were analyzed by Dixon plot. The reaction velocity was measured at a fixed concentration of substrate, while concentration of the inhibitor was varied. The K_i values for the inhibitors were calculated from the x-intercept of the Dixon plot. All the

Chart 1. Scaffolds Tested against PfENR

1,3,4-oxadiazole
(7 Compounds)

4,5-dihydro-1H-pyrazole
(6 Compounds)

1,2,5,6-Tetrahydropyrimidine
(2 Compounds)

1H-pyrrole-2,5-dione
(7 Compounds)

1H-1,2,4-triazole
(3 Compounds)

1H-imidazol-2(3H)-one
(12 Compounds)

2H-Pyrano[2,3-c]pyridin-2-imine
(4 Compunds)

Quinazolin-4(3H)-one
(6 Compounds)

Thiazolidine-4-carboxylic acid
(14 Compounds)

1H-imidazole-2-thiol
(2 Compounds)

4-Aminothiazole-2(3H)-thione
(3 Compounds)

Quinazolin-4-amine
(15 Compounds)

Isoxazole
(15 Compounds)

Thiophene
(6 Compounds)

2,3-Dihydro-1H-quinazolin-4-one
(4 Compounds)

4H-1,2,4-triazole
(4 Compounds)

5-Methylene-2-thioxothiazolidin-4-one
(30 Compounds)

4-Methyleneoxazol-5(4H)-one
(16 Compounds)

5-Methylene-2-thioxoimidazolidin-4-one
(2 Compounds)

Thiazolidin-5-one
(1 Compound)

2H-Pyrano[2,3-c]pyridin-2-one
(1 Compound)

H-imidazo[1,2-a]pyridine
(17 Compounds)

6,11a-dihydro-4aH-indolo[2,3-b]quinoxaline
(3 Compounds)

1,2,4-triazine-3,5(2H,4H)-dione
(2 Compounds)

Thiourea
(11 Compounds)

Quinoline
(75 Compounds)

Thieno[3,2-d]pyrimidine-2,4(1H,3H)-dione
(2 Compounds)

Diaryl ethers
(25 Compounds)
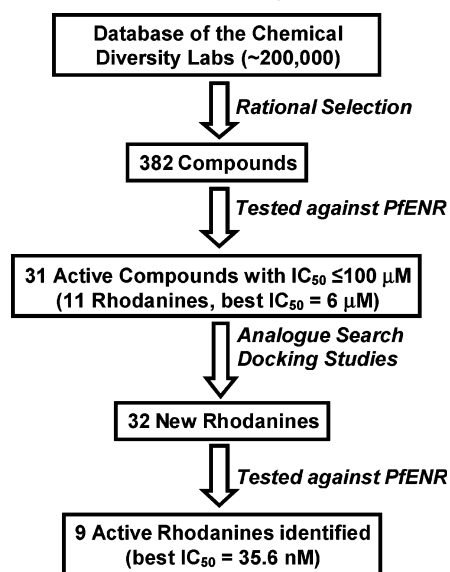
Diarylaza ethers
(2 Compounds)

rhodanines were competitive inhibitors for crotonoyl-CoA (Figure 1b) and exhibited noncompetitive inhibition for NADH (Figure 1c). The K_i values of these inhibitors with respect to both crotonoyl-CoA and NADH are given in Tables 1, 2 and 3 along with their respective IC_{50} values. The kinetics of the rhodanine compounds clearly indicate that these compounds occupy either the substrate binding site or a site overlapping with it, thus blocking the enzyme activity by forbidding the entry of the substrate to the active site of the enzyme. Thus, a K_i value for compound **17** was calculated to be 4.2 nM against crotonoyl-CoA (Figure 1b) and 32.7 nM against NADH (Figure 1c). Triclosan exhibits uncompetitive kinetics for crotonoyl-CoA and yields a K_i value of 660 nM. Thus, the rhodanines not only follow a different mechanism to inhibit PfENR but also the best among them (compound **17**) is almost 13 times more potent than triclosan.

***In Vitro* Whole-Cell Assay against *P. falciparum*.** Antimalarial activity of the best rhodanine inhibitor of PfENR (**17**) was checked against the chloroquine-sensitive *P. falciparum* FCK2 strain in red blood cell cultures. The IC_{50} value for growth inhibition of the parasite was found to be ~0.75 μM by nonlinear regression analysis after 96 h (Figure 1d), which is quite significant. The minimum inhibitory concentration value of the compound was found to be 2.5 μM. From the inhibitory data of *P. falciparum* cultured in human erythrocytes, it is evident that compound **17** is as potent as triclosan[3] in inhibiting the parasite growth.

Thus, both from enzyme inhibition data and from the in vitro *Plasmodium* growth inhibition studies, it is concluded that compound **17** of the rhodanine series provides a promising lead compound for the development of a novel series of rhodanine-based antiplasmodium chemotherapeutics.
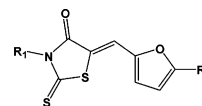
Scheme 2. Flow Chart for This Study

Table 1. Inhibitory Potencies of the 5-((Furan-2-yl)methylene)-2-thioxothiazolidin-4-one Class of Compounds for PfENR

Compound No.	R$_1$	R$_2$	IC$_{50}$ (μM)	K$_i^a$ (μM)	K$_i^b$ (μM)
1	H		0.87	0.48	0.56
2	H		0.98	0.51	0.63
3	H		1.7	0.88	1.05
4	H		6.0	2.0	2.5
5	H		6.1	4.1	5.5
6			20.0	n.d.	n.d.
7	H		28.5	n.d.	n.d.
8	CH$_3$		30.25	n.d.	n.d.
9	H		35.0	n.d.	n.d.
10			>100	n.d.	n.d.
11		H	>100	n.d.	n.d.
12			>100	n.d.	n.d.
13	CH$_3$		>100	n.d.	n.d.
14	CH$_3$		Insoluble	n.d.	n.d.
15	CH$_3$		n.i.	n.d.	n.d.
16	CH$_3$		Ppt.	n.d.	n.d.

^{a} With respect to crotonoyl CoA. ^{b} With respect to NADH.

Structure−Activity Relationship of 5-((Furan-2-yl)methylene)-2-thioxothiazolidin-4-one Compounds: There were 16 compounds belonging to this series in our acquired library of 414 compounds. Out of these 16 compounds (**1−16**), nine gave IC$_{50}$ values of less than 35 μM (**1−9**), and the best among this class of molecules is compound **1** with an IC$_{50}$ of 0.87 μM. It has an H at R$_1$ and a 2,3-dichloro-phenyl at R$_2$. Any replacement of R$_1$ with a bigger group led to a decrease in inhibitory activity (e.g., compound **8**). At R$_2$, displacement of the chlorine from position-3 to any other position also led to a decrease in activity (compound **9**). Moving the chlorine from position-2 to position-4 has also led to a slight decrease in activity (compound **2**). Removal of this chlorine altogether reduces the inhibitory activity further (compound **3**). Also, its replacement at the *para*-position by a methyl group led to a further diminution in activity (compound **7**). Likewise, replacement of R$_1$ with a methyl group not only reduces the activity of the compound, it also makes the compound more hydrophobic and in general insoluble in most solvents (compound **14**). IC$_{50}$ values of all the compounds in this series are given in Table 1.

Docking studies with AutoDock show that in the case of R$_1$ = H, the thioxothiazolidin-4-one core moiety occupies the same space in the substrate binding site as does the ring A of triclosan and makes a stacking interaction with the nicotinamide ring of NAD$^+$ (Figure 2b). This stacking interaction is very important and has been conserved in all the ENRs for which the crystal structures have been solved with NAD$^+$ and triclosan in ternary complex with the enzyme. The oxygen of this core moiety makes hydrogen bonds with the OH of the active site Tyr^{277} as well as the NO$_2$* of nicotinamide ribose. This interaction is also conserved in all the ternary complexes of ENR−NAD$^+$−triclosan solved so far. The docked compounds also explain the importance of H at R$_1$. The NH group makes NH−π interaction with the aromatic side chain of Tyr^{267}. Replacement of H with any bigger group will lead to a steric clash with the side chain of Tyr^{267} and, hence, we observe a decrease in activity when H is replaced with CH$_3$ (compound **8**). At R$_2$, the chlorine on the benzene ring at the *meta*-position (compound **1**) make hydrophobic−hydrophobic contacts with AC8, AC2*, AC3*, and AC5* of NAD. But there is also an unfavorable hydrophobic−hydrophilic contact with O of Ala^{217}. Given the hydrophilic nature of this part of the active site, any more additions of chlorines lead to unfavorable interactions and, hence, a decrease
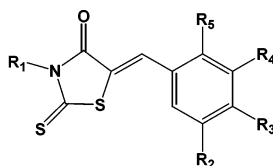
in inhibitory activity. Probably an OH at the *para*-position would be a better replacement, which could make hydrogen bonds with the backbone O of Ala^{217} or the side chain of Asn218 (Figure 2b). The one exceptional compound (compound **6**) that shows moderate activity even with a bigger R$_1$ binds at the active site in a different manner compared to other active compounds of this series.

Structure−Activity Relationship of 5-Benzylidene-2-thioxothiazolidin-4-one Compounds: In our acquired library of 414 compounds, there were 35 compounds belonging to this

Table 2. Inhibitory Potencies of the 5-Benzylidene-2-thioxothiazolidin-4-one Class of Compounds with Aromatic R_1 for PfENR[a]

Compd. No	R_1	R_2	R_3	R_4	R_5	IC_{50} (µM)	K_i^b (µM)	K_i^c (µM)
17	phenyl	OH	OH	H	H	0.035	.0042	.032
18	4-OH-phenyl	H	OCH$_3$	H	H	10.0	8.7	9.1
19	4-OCH$_3$-phenyl	H	CHO	H	H	12.5	13.2	14.4
20	4-OH-phenyl	H	Cl	H	Cl	25.0	n.d.	n.d.
21	4-OH-phenyl	H	N(CH$_3$)$_2$	H	H	25.0	n.d.	n.d.
22	4-OH-phenyl	OCH$_3$	OH	H	H	30.0	n.d.	n.d.
23	4-OCH$_3$-phenyl	H	OCH$_3$	fused ring (R$_5$, R$_4$)	-	98.58	n.d.	n.d.
24	4-N(diethyl)-phenyl	H	OCH$_3$	H	H	>50^d	n.d.	n.d.
25	4-OCH$_3$-phenyl	ring (R$_6$, R$_2$)	H	ring (R$_5$, R$_4$)	-	>50^d	n.d.	n.d.
26	4-F-phenyl	OH	H	H	H	>100	n.d.	n.d.
27	phenyl	OH	H	H	H	>100	n.d.	n.d.
28	4-OCH$_3$-phenyl	H	OCH$_3$	H	H	>100	n.d.	n.d.
29	4-OCH$_3$-phenyl	H	CH$_3$	H	H	insoluble	n.d.	n.d.
30	4-OCH$_3$-phenyl	H	CH(CH$_3$)$_2$	H	H	>100	n.d.	n.d.
31	4-OCH$_3$-phenyl	H	N(CH$_3$)$_2$	H	H	>100	n.d.	n.d.
32	4-OCH$_3$-phenyl	H	H	H	H	>100	n.d.	n.d.
33	4-OCH$_2$CH$_3$-phenyl	H	H	ring (R$_5$, R$_4$)	-	n.i	n.d.	n.d.
34	3-CH$_3$-phenyl	H	OH	H	H	Insoluble	n.d.	n.d.
35	3,4-dimethyl-phenyl	H	OCH$_3$	H	H	Insoluble	n.d.	n.d.

[a] R_6 = H except in entry 37. [b] With respect to crotonoyl-CoA. [c] With respect to NADH. [d] Insoluble above 50 µM.

Table 3. Inhibitory Potencies of the 5-Benzylidene-2-thioxothiazolidin-4-one Class of Compounds with Aliphatic R_1 for PfENR

Compd No	R_1	R_2	R_3	R_4	R_5	IC_{50} (μM)	K_i^a (μM)	K_i^b (μM)
36	(aliphatic chain, COOH)	OCH_3	(O-benzyl, Cl)	H	H	6.5	5.1	5.4
37	(aliphatic chain, COOH)	OCH_3	(O-pentyl)	H	H	7.0	6.6	7.3
38	(aliphatic chain, COOH)	OCH_3	(O-propyl)	H	H	45.0	n.d.	n.d.
39	(aliphatic chain, COOH)	H	(isopropyl)	H	H	>100	n.d.	n.d.
40	(CH_3)	H	(N,N-diethylaminomethyl)	H	OH	>100	n.d.	n.d.
41	(CH_3)	Cl	OH	Cl	H	>100	n.d.	n.d.
42	(aliphatic chain, $COOCH_3$)	H	(CH_3)	H	H	>100	n.d.	n.d.
43	(aliphatic chain, $COOCH_3$)	OH	H	H	H	>100	n.d.	n.d.
44	(aliphatic chain, $COOCH_3$)	H	Cl	H	H	>100	n.d.	n.d.
45	(aliphatic chain, COOH)	OCH_3	(O-pentyl)	H	H	>100	n.d.	n.d.
46	(O-CH2CH2-N(CH3)2 ester)	H	Cl	H	Cl	>100	n.d.	n.d.
47	(N(CH3)-CH2CH2-O ester)	H	H	H	H	>100	n.d.	n.d.
48	(aliphatic chain, COOH)	CH_3	(O-benzyl)	H	H	>100	n.d.	n.d.
49	(aliphatic chain, $COOCH_3$)	H	Br	H	H	Insoluble	n.d.	n.d.
50	(aliphatic chain, $COOCH_3$)	H	(O-butyl)	H	H	n.i	n.d.	n.d.
51	(aliphatic chain, $COOCH_3$)	OCH_3	OCH_3	OCH_3	H	n.i	n.d.	n.d.

[a] With respect to crotonoyl-CoA. [b] With respect to NADH.

series. This series could be further divided into two subcategories, one with a six-carbon aromatic ring and the other with an aliphatic chain at R_1, which is attached to the nitrogen of 2-thioxothiazolidin-4-one core moiety (Tables 2 and 3). Nineteen compounds belonged to the first subcategory (with an aromatic ring at R_1). Out of these, six compounds (**17**–**22**) showed an IC_{50} of ≤30 μM. Compound **17** (mol wt 329.399) with an IC_{50} value of 35.6 nM against 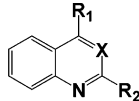PfENR was the most potent of all the compounds tested. Overall, 10 compounds (**17**–**23** and **36**–**38**) gave IC_{50} values lesser than 100 μM, while 21 compounds (**24**–**28**, **30**–**33**, **39**–**48**, **50**, and **51**) did not show any significant inhibition up to a concentration of 100 μM. Four compounds (**29**, **34**, **35**, and **49**) in this series did not dissolve in water/DMSO. IC_{50} values of all the compounds in this series are given in Tables 2 and 3. Looking into the structure–activity relationship of the first subcategory of compounds, we find that

the compound having a phenyl group at R_1 and hydroxyl groups at R_2 and R_3 (**17**) is relatively more effective of all the molecules of this class investigated in these studies. Hydroxyl group at R_3 seems to be the most critical factor for activity, replacement of this hydroxyl group with hydrogen led to a total abolition of inhibitory activity (compound **24**, $IC_{50} > 100$). Docking studies show that compounds belonging to this subcategory bind in a different manner compared to the earlier series of rhodanines. In this case, it is the phenyl ring attached to the 2-thioxothia-zolidin-4-one core moiety through a methylene bridge (equivalent to the furan of the earlier class of compounds) that shows stacking interaction with the nicotinamide of NAD^+, though the oxygen of the 2-thioxothiazolidin-4-one moiety still makes hydrogen bond with the OH of Tyr^{277} of the active site (Figure 2c). All inhibitors of this subcategory bind in a similar fashion, and the docked complex of compound **17** is shown in Figure 2b as a model case. There are two new hydrogen bonds, the *m*-OH on the phenyl ring that stacks over nicotinamide ring of NAD^+, participating in a hydrogen bond with C=O of Ala^{320}, and the *p*-OH makes a hydrogen bond with the side chain of Tyr^{267}. These additional hydrogen bonds are probably the reason for high inhibitory activity of this compound.

The compounds in the other subcategory of this series mostly have aliphatic chains, some ending with $-COOH/-COOCH_3$ at R_1, having $OH/Cl/OCH_3$ at R_2 and an aromatic group or an aliphatic chain linked through an ether at R_3 (Table 3). Out of 18 compounds in this subcategory, only three were active at <50 μM. Best among them gave IC_{50} values of 6.5 and 7.0 μM (compounds **36** and **37**). The third one gave an IC_{50} of 45.0 μM (compound **38**). These three compounds differ at R_3, while compound **36** has a *p*-chlorobenzene, compounds **37** and **38** have five- and two-carbon alkyl chains, respectively. Shortening of the aliphatic chain by three carbons (**38**) led to a 6.4-fold decrease in inhibitory activity. Surprisingly, compound **45** with a corresponding intermediate length of four carbon chain did not show inhibition even at 100 μM. Docked complex of compound **36** with PfENR shows stacking interactions of *p*-chlorobenzene at R_2 with the nicotinamide ring of NAD^+. The C=O of the rhodanine core moiety is involved in hydrogen bonding with NH of Asn^{218} and the COOH at R_1 is involved in hydrogen bonding with the side chains of Asp^{236} and Lys^{240} (Figure 2d), but due to a large number of possible torsions in the aliphatic chain of the molecule, the conformations do not cluster well together. Cluster analysis shows that there are only five to seven conformations in the most populated clusters in a set of 100 runs, and much of the variations are contributed by the highly flexible aliphatic chain at R_1.

Structure–Activity Relationship of the Quinoline/Quinazo-line Class of Compounds: These compounds exhibited moderate activity and were much poorer as inhibitors compared to rhodanines. We had three compounds with quinoline (X = CH) and one compound with quinazoline (X = N) as core moiety in our library. Both R_1 and R_2 groups as well as the core moieties are dominated by ring structures, and hence, $\pi-\pi$ stacking interactions are expected to play a major role in their affinity towards PfENR. The first quinoline (**53**) with a 1,2,3,4-tetrahydro-naphthalene group attached through a methyl-acet-amide at R_1 and 1-chloro-3-methylsulfanyl-benzene at R_2 gave an IC_{50} value of 50.0 μM. In the other two quinolines, there is a common group, 2-chloro-thiophene, at R_2 but different groups at R_1. Compound **55** has 1-chloro-4-methoxy-benzene and compound **56** has 1-propyl-1,2,3,4-tetrahydro-quinoline linked through a methyl-acetamide at R_1. Both of these compounds have an IC_{50} value of 60 μM. The quinazoline compound (**54**)

Table 4. Inhibitory Potencies of the Quinoline/Quinazoline Class of Compounds for PfENR

Compd. No	X	R_1	R_2	IC_{50} (μM)
53	CH			50.0
54	N			52.0
55	CH			60.0
56	CH			60.0

with a (4-chloro-benzyl)-methyl-amine group at R_1 and 1-chloro-4-methylsulfanylmethyl-benzene group at R_2 gave an IC_{50} of 52.0 μM (Table 4).

Other than these three series of compounds, there were four sets of two compounds each (**57–64**) that gave IC_{50} values ranging from 40.0 to 100 μM (Supporting Information).

Conclusion

Small-molecule databases present an ocean of scaffolds from which representative compounds can be tested for their inhibitory activity against a desired drug target to find new class of lead inhibitors. Based on the information gathered from our previous structural studies on the active site of PfENR and the interactions in the PfENR–NAD^+–triclosan complex, we identified ~20 such compounds. These compounds inhibit PfENR at nanomolar to micromolar concentrations, and the most potent of them has an IC_{50} of 35.6 nM in spectrophotometric assay. This compound (**17**) also inhibits *Plasmodium* growth in red blood cell cultures with an IC_{50} of ~0.75 μM, making this class of compounds promising candidates for further evaluation in *in vivo* studies. Inhibition kinetics were deduced for the top 10 inhibitors and they are found to be competitive inhibitors with respect to substrate. Most of the inhibitors belong to 2-thioxothiazolidin-4-one class of compounds, also known as rhodanines. The *in vitro* inhibition constants of compound **17** are better than the well proven antimalarial agent triclosan, which further underscores the importance of the current study. Molecular docking studies show that many of the active compounds bind at the substrate binding site of PfENR in a fashion similar to triclosan, show stacking interactions with the cofactor NAD^+ and similar hydrogen bonding as found in the case of triclosan. Thus, our strategy to exploit the knowledge about interactions in the PfENR–NAD^+–triclosan complex has proven successful leading to the discovery of a novel class of PfENR inhibitors. Libraries of this class of compounds could be screened *in silico* to explore further PfENR inhibitors and establish a structure–activity relationship leading to a pharma-cophore model.

Experimental Section

Compounds of the Chemical Diversity Labs: All compounds tested were obtained from Chemical Diversity Labs, California and Moscow. The compounds are >93–95% pure, and the nuclear

magnetic resonance (NMR) spectra of compounds provided by the supplier are given in the Supporting Information. The ESI-MS data were obtained on a Waters' Micromass LCT mass spectrometer equipped with a TOF analyzer, MassLynx data system, and pneumatic-nebulizer-assisted electrospray LC/MS interface. Acetonitrile−water (1:1 mixture) was used as carrier solvent at a flow rate of 50 μL min^{-1}. The samples were dissolved in DMSO to get concentrations in micromolar range, and 5 μL of each sample was injected. Desolvation gas (grade-1 nitrogen) was used at a flow rate of 400 L h^{-1} and maintained at 150 °C, while nebulizer gas (grade-1 nitrogen) was used at fully opened port. A capillary voltage of 3500 V was used against the cone voltage of 40 V. The MCP detector was kept at 2600.

Materials for PfENR Preparation and Enzyme Assay: Media components were obtained from Hi-media (Delhi, India) β-NADH, crotonoyl-CoA, imidazole, DMSO, and SDS/PAGE reagents were bought from Sigma. All other chemicals were of analytical grade.

Expression and Purification of Recombinant PfENR: PfENR was expressed and purified as described previously.[11] The plasmid with the 6XHis-tagged gene coding for the enzyme was transformed into BL21 (DE3) cells. Culture was grown at 37 °C for 12 h, followed by subsequent purification on Ni−NTA (Ni^{2+}−nitrilo-acetate)−agarose column using an imidazole gradient. PfENR was eluted using 400 mM imidazole. The purity of the protein was confirmed by SDS/PAGE.

Enzyme Assay: Enoyl-ACP reductase from *P. falciparum* was assayed using spectrophotometric method at 25 °C by monitoring the decrease in the absorbance of NADH at 340 nm. The standard reaction mixture, in a total volume of 100 μL, contained 150 mM Tris-NaCl buffer (pH 7.5), 200 μM crotonoyl-CoA, 100 μM NADH, 200 nM enzyme, and 1% DMSO. A 10 mM stock solution of the inhibitors was made in DMSO. The stocks were serially diluted to add to the final reaction mixture for inhibition studies. The reaction proceeds by reduction of crotonoyl-CoA to butyryl-CoA with the oxidation of NADH to NAD$^+$, which is monitored at 340 nm. Data points were the mean of three different sets of experiments, and the individual values were within ±10% of the average.

Determination of IC$_{50}$ Values: IC$_{50}$ values of the synthesized compounds for ENRs were determined by measuring the ENR activity at various concentrations of these compounds. In the standard reaction mixture mentioned above, various concentrations of the compounds of interest were added one by one, and the percent inhibition was calculated from the residual enzymatic activity. The percent activity thus calculated was plotted against log concentration of the compound. The data were analyzed by nonlinear regression method using SigmaPlot 6.0 and the value of IC$_{50}$ determined from the fit of the data (IC$_{50}$ corresponds to the concentration of the compound that inhibited ENR activity by 50%).

Determination of K_i: K_i of individual inhibitors were determined with respect to NADH and crotonoyl-CoA in separate experiments. With respect to NADH, data were collected against two fixed concentrations of NADH (50 μM and 100 μM), while varying the inhibitor concentration from 1 nM to their respective IC$_{50}$ values and keeping crotonoyl-CoA concentration fixed at 200 μM. For K_i with respect to crotonoyl-CoA, data were collected against two fixed concentrations of crotonoyl-CoA (100 μM and 200 μM) and inhibitor concentration was varied from 1 nM to the IC$_{50}$ value, while NADH concentration was kept at 100 μM. All the data were analyzed using the Dixon plot.[43]

Parasite Culture and Growth Inhibition Assay: The experiments were performed using *P. falciparum* FCK2 strain (chloro-quine-sensitive, IC$_{50}$=18 nM), an isolate from Karnataka, India. *P. falciparum* was cultured using standard techniques[44] and routinely synchronized using 5% sorbitol[45] at 4% hematocrit in RPMI 1640 (Invitrogen, Carlsbad, CA) medium supplemented with 10% human serum, 0.225% sodium bicarbonate, and 0.01 mg/mL gentamycin. Growth inhibition was monitored using direct microscopic examination of the parasite by standard Giemsa staining. Typically uninfected or infected (1−2% parasitemia) red blood cells (2% hematocrit) were added to the culture medium in the wells of a 96-well plate (Nunc, Roskilde, Denmark), and a different concen-

tration of inhibitor in Me$_2$SO did not exceed 0.05%. The experiment started with the synchronized parasite culture in the early trophozoite stage, and inhibitors were added up to the fourth day. Solvent controls as well as triclosan as positive control were included. *P. falciparum* growth was compared with solvent control. The IC$_{50}$ was calculated from a plot of relative percent parasitemia versus log concentration of the inhibitor by fitting it to nonlinear regression analysis using SigmaPlot 2000 software (Systat Software Inc., CA).

Docking Studies of Inhibitors with PfENR: Preparation of the Ligand and Receptor Molecules for Docking Studies: Docking simulations were done using the program Autodock version 3.05. The crystal structure of PfENR submitted to PDB (www.rcsb.org) by Pidugu et al.[16] was used for docking experiments. Hydrogens were added and energy minimized. The 3-d coordinates were converted into the mol2 format with MMFF94 charges using the MOE (Molecular Operating Environment) suite of programs.[46] The script molto2pdbqs (provided with AutoDock program) was used to make the receptor file containing data on fractional volumes and solvation parameters. Ligands were built using MOE and energy minimized with MMFF94 charges. The script AutoTors (provided with AutoDock program) was used to define torsion angles in the ligands prior to docking.

Docking Simulations: All docking simulations were done with AutoDock.[47,48] Briefly, grid maps for docking simulations were generated with 81 grid points (with 0.375 Å spacing) in the *x*, *y*, and *z* direction centered in the active site using the AutoGrid program. Lennard−Jones parameters 12-10 and 12-6 (supplied with the program package) were used for modeling H-bonds and van der Waals interactions, respectively. The distance-dependent di-electric permittivity of Mehler and Solmajer[49] was used in the calculations of the electrostatic grid maps. The Genetic algorithm (GA) and Lamarckian genetic algorithm with the pseudo Solis and Wets modification (LGA/pSW) methods were used with default parameters. Each docking experiment consisted of a series of 100 simulations. Cluster analysis was performed on the results using an RMS tolerance of 2.0 Å.

Supporting Information Available: A table of compounds with moderate activity against PfENR and spectral data and elemental analyses of the best 10 of the rhodanine compounds. This material is available free of charge via the Internet at http://pubs.acs.org.

References

(1) WHO World Malaria Report, 2005; World Health Organization: Geneva, Switzerland (http://rbm.who.int/wmr2005).
(2) Mutabingwa, T. K.; Anthony, D.; Heller, A.; Hallett, R.; Ahmed, J.; Drakeley, C.; Greenwood, B. M.; Whitty, C. J. Amodiaquine alone, amodiaquine+sulfadoxine-pyrimethamine, amodiaquine+artesunate, and artemether-lumefantrine for outpatient treatment of malaria in Tanzanian children: A four-arm randomised effectiveness trial. *Lancet* **2005**, *365*, 1474−1480.
(3) Surolia, N.; Surolia, A. Triclosan offers protection against blood stages of malaria by inhibiting enoyl-ACP reductase of Plasmodium falciparum. *Nature Med.* **2001**, *7*, 167−173.
(4) Rock, C. O.; Cronan, J. E. *Escherichia coli* as a model for the regulation of dissociable (type II) fatty acid biosynthesis. *Biochim. Biophys. Acta* **1996**, *1302*, 1−16.
(5) Smith, S.; Witkowski, A.; Joshi, A. K. Structural and functional organization of the animal fatty acid synthase. *Prog. Lipid Res.* **2003**, *42*, 289−317.
(6) Ralph, S. A.; Van Dooren, G. G.; Waller, R. F.; Crawford, M. J.; Fraunholz, M. J.; Foth, B. J.; Tonkin, C. J.; Roos, D. S.; McFadden, G. I. Tropical infectious diseases: Metabolic maps and functions of the *Plasmodium falciparum* apicoplast. *Nat. Rev. Microbiol.* **2004**, *2*, 203−216.
(7) Heath, R. J.; Rock, C. O. Enoyl-acyl carrier protein reductase (fabI) plays a determinant role in completing cycles of fatty acid elongation in Escherichia coli. *J. Biol. Chem.* **1995**, *270*, 26538−26542.

(8) Wiesner, J.; Seeber, F. The plastid-derived organelle of protozoan human parasites as a target of established and emerging drugs. *Expert Opin. Ther. Targets* **2005**, *9*, 23−44.

(9) Zhang, Y. M.; Lu, Y. J.; Rock, C. O. The reductase steps of the type II fatty acid synthase as antimicrobial targets. *Lipids* **2004**, *39*, 1055−1060.

(10) Moir, D. T. Identification of inhibitors of bacterial enoyl-acyl carrier protein reductase. *Curr. Drug Targets Infect. Disord.* **2005**, *5* (3), 297−305.

(11) Kapoor, M.; Dar, M. J.; Surolia, A.; Surolia, N. Kinetic determinants of the interaction of enoyl-ACP reductase from Plasmodium falciparum with its substrates and inhibitors. *Biochem. Biophys. Res. Commun.* **2001**, *289*, 832−837.

(12) Kapoor, M.; Reddy, C. C.; Krishnasastry, M. V.; Surolia, N.; Surolia, A. Slow-tight-binding inhibition of enoyl-acyl carrier protein reductase from *Plasmodium falciparum* by triclosan. *Biochem. J.* **2004**, *381*, 719−24.

(13) Kapoor, M.; Mukhi, M. L.; Surolia, N.; Suguna, K.; Surolia, A. Kinetic and structural analysis of the increased affinity of enoyl-ACP (acyl-carrier protein) reductase for triclosan in the presence of NAD$^+$. *Biochem. J.* **2004**, *381*, 725−733.

(14) Kapoor, M.; Gopalakrishnapai, J.; Surolia, N.; Surolia, A. Mutational analysis of the triclosan-binding region of enoyl-ACP (acyl-carrier protein) reductase from *Plasmodium falciparum*. *Biochem. J.* **2004**, *381*, 735−741.

(15) Suguna, K.; Surolia, A.; Surolia, N. Structural basis for triclosan and NAD binding to enoyl-ACP reductase of *Plasmodium falciparum*. *Biochem. Biophys. Res. Commun.* **2001**, *283* (1), 224−228.

(16) Pidugu, L. S.; Kapoor, M.; Surolia, N.; Surolia, A.; Suguna, K. Structural basis for the variation in triclosan affinity to enoyl reductases. *J. Mol. Biol.* **2004**, *343*, 147−155.

(17) Perozzo, R.; Kuo, M.; Sidhu, A. S.; Valiyaveettil, J. T.; Bittman, R.; Jacobs, W. R., Jr.; Fidock, D. A.; Sacchettini, J. C. Structural elucidation of the specificity of the antibacterial agent triclosan for malarial enoyl acyl carrier protein reductase. *J. Biol. Chem.* **2002**, *277* (15), 13106−13114.

(18) Sharma, S.; Ramya, T. N. C.; Surolia, A.; Surolia, N. Triclosan as a systemic antibacterial agent in a mouse model of acute bacterial challenge. *Antimicrob. Agents Chemother.* **2003**, *47*, 3859−3866.

(19) Chhibber, M.; Kumar, G.; Parasuraman, P.; Ramya, T. N.; Surolia, N.; Surolia, A. Novel diphenyl ethers: Design, docking studies, synthesis, and inhibition of enoyl ACP reductase of *Plasmodium falciparum* and *Escherichia coli. Bioorg. Med. Chem.* **2006**, *14* (23), 8086−8098.

(20) Freundlich, J. S.; Yu, M.; Lucumi, E.; Kuo, M.; Tsai, H. C.; Valderramos, J. C.; Karagyozov, L.; Jacobs, W. R., Jr.; Schiehser, G. A.; Fidock, D. A.; Jacobus, D. P.; Sacchettini, J. C. Synthesis and biological activity of diaryl ether inhibitors of malarial enoyl acyl carrier protein reductase. Part 2: 2′-substituted triclosan derivatives. *Bioorg. Med. Chem. Lett.* **2006**, *16*, 2163−2169.

(21) Freundlich, J. S.; Anderson, J. W.; Sarantakis, D.; Shieh, H. M.; Yu, M.; Valderramos, J. C.; Lucumi, E.; Kuo, M.; Jacobs, W. R., Jr.; Fidock, D. A.; Schiehser, G. A.; Jacobus, D. P.; Sacchettini, J. C. Synthesis, biological activity, and X-ray crystal structural analysis of diaryl ether inhibitors of malarial enoyl acyl carrier protein reductase. Part 1: 4′-Substituted triclosan derivatives. *Bioorg. Med. Chem. Lett.* **2005**, *15*, 5247−5252.

(22) Kumar, S.; Kumar, G.; Kapoor, M.; Surolia, A.; Surolia, N. Synthesis and evaluation of substituted pyrazoles: Potential antimalarials targeting the enoyl ACP reductase of *Plasmodium falciparum. Synth. Commun.* **2006**, *36* (2), 215−226.

(23) Sharma, S. K.; Prasanna, P.; Kumar, G.; Surolia, N.; Surolia, A. Green tea catechins potentiate triclosan binding to enoyl-ACP reductase from *Plasmodium falciparum* (PfENR). *J. Med. Chem.* **2007**, *50*, 765−775.

(24) Bruno, G.; Costantino, L.; Curinga, C.; Maccari, R.; Monforte, F.; Nicolo, F.; Ottana, R.; Vigorita, M. G. Synthesis and aldose reductase inhibitory activity of 5-arylidene-2,4-thiazolidinediones. *Bioorg. Med. Chem. Lett.* **2002**, *10*, 1077−1084.

(25) Grant, E. B.; Guiadeen, D.; Baum, E. Z.; Foleno, B. D.; Jin, H.; Montenegro, D. A.; Nelson, E. A.; Bush, K.; Hlasta, D. J. The synthesis and SAR of rhodanines as novel class C beta-lactamase inhibitors. *Bioorg. Med. Chem. Lett.* **2000**, *10*, 2179−2182.

(26) Momose, Y.; Meguro, K.; Ikeda, H.; Hatanaka, C.; Oi, S.; Sohda, T. Studies on antidiabetic agents. X. Synthesis and biological activities of pioglitazone and related compounds. *Chem. Pharm. Bull. (Tokyo)* **1991**, *39* (6), 1440−1445.

(27) Sim, M. M.; Ng, S. B.; Buss, A. D.; Crasta, S. C.; Goh, K. L.; Lee, S. K. Benzylidene rhodanines as novel inhibitors of UDP-N-acetylmuramate/L-alanine ligase. *Bioorg. Med. Chem. Lett.* **2002**, *12*, 697−699.

(28) Whitesitt, C. A.; Simon, R. L.; Reel Jon, K.; Sigmund, S. K.; Phillips, M. L.; Shadle, J. K.; Heinz, L. J.; Koppel, G. A.; Hundel, D. C.; Lifer, S. L.; Berry, D.; Ray, J.; Little, S. P.; Liu, X.; Marshall, W. S.; Panetta, J. A. Synthesis and structure−activity relationships of benzophenones as inhibitors of cathepsin D. *Bioorg. Med. Chem. Lett.* **1996**, *6*, 2157−2162.

(29) Free, C. A.; Majchrowicz, E.; Hess, S. M. Mechanism of inhibition of histidine decarboxylase by rhodanines. *Biochem. Pharm.* **1971**, *20*, 1421−1428.

(30) Vilcheze, C.; Wang, F.; Arai, M.; Hazbon, M. H.; Colangeli, R.; Kremer, L.; Weisbrod, T. R.; Alland, D.; Sacchettini, J. C.; Jacobs, W. R., Jr. Transfer of a point mutation in Mycobacterium tuberculosis inhA resolves the target of isoniazid. *Nat. Med.* **2006**, *12* (9), 1027−1029.

(31) Heerding, D. A.; Chan, G.; DeWolf, W. E.; Fosberry, A. P.; Janson, C. A.; Jaworski, D. D.; McManus, E.; Miller, W. H.; Moore, T. D.; Payne, D. J.; Qiu, X.; Rittenhouse, S. F.; Slater-Radosti, C.; Smith, W.; Takata, D. T.; Vaidya, K. S.; Yuan, C. C.; Huffman, W. F. 1,4-Disubstituted imidazoles are potential antibacterial agents functioning as inhibitors of enoyl acyl carrier protein reductase (FabI). *Bioorg. Med. Chem. Lett.* **2001**, *11* (16), 2061−2065.

(32) Miller, W. H.; Seefeld, M. A.; Newlander, K. A.; Uzinskas, I. N.; Burgess, W. J.; Heerding, D. A.; Yuan, C. C.; Head, M. S.; Payne, D. J.; Rittenhouse, S. F.; Moore, T. D.; Pearson, S. C.; Berry, V.; DeWolf, W. E., Jr.; Keller, P. M.; Polizzi, B. J.; Qiu, X.; Janson, C. A.; Huffman, W. F. Discovery of aminopyridine-based inhibitors of bacterial enoyl-ACP reductase (FabI). *J. Med. Chem.* **2002**, *45* (15), 3246−3256.

(33) Levy, C. W.; Baldock, C.; Wallace, A. J.; Sedelnikova, S.; Viner, R. C.; Clough, J. M.; Stuitje, A. R.; Slabas, A. R.; Rice, D. W.; Rafferty, J. B. A study of the structure−activity relationship for diazaborine inhibition of *Escherichia coli* enoyl-ACP reductase. *J. Mol. Biol.* **2001**, *309* (1), 171−180.

(34) Ohishi, Y.; Mukai, T.; Nagahara, M.; Yajima, M.; Kajikawa, N.; Miyahara, K.; Takano, T. Preparations of 5-alkylmethylidene-3-carboxymethylrhodanine derivatives and their aldose reductase inhibitory activity. *Chem. Pharm. Bull. (Tokyo)* **1990**, *38* (7), 1911−1919.

(35) Sing, W. T.; Lee, C. L.; Yeo, S. L.; Lim, S. P.; Sim, M. M. Arylalkylidene rhodanine with bulky and hydrophobic functional group as selective HCV NS3 protease inhibitor. *Bioorg. Med. Chem. Lett.* **2001**, *11* (2), 91−94.

(36) Orchard, M. G.; Neuss, J. C.; Galley, C. M.; Carr, A.; Porter, D. W.; Smith, P.; Scopes, D. I.; Haydon, D.; Vousden, K.; Stubberfield, C. R.; Young, K.; Page, M. Rhodanine-3-acetic acid derivatives as inhibitors of fungal protein mannosyl transferase 1 (PMT1). *Bioorg. Med. Chem. Lett.* **2004**, *14* (15), 3975−3978.

(37) Ahn, J. H.; Kim, S. J.; Park, W. S.; Cho, S. Y.; Ha, J. D.; Kim, S. S.; Kang, S. K.; Jeong, D. G.; Jung, S. K.; Lee, S. H.; Kim, H. M.; Park, S. K.; Lee, K. H.; Lee, C. W.; Ryu, S. E.; Choi, J. K. Synthesis and biological evaluation of rhodanine derivatives as PRL-3 inhibitors. *Bioorg. Med. Chem. Lett.* **2006**, *16* (11), 2996−2999.

(38) Cutshall, N. S.; O'Day, C.; Prezhdo, M. Rhodanine derivatives as inhibitors of JSP-1. *Bioorg. Med. Chem. Lett.* **2005**, *15* (14), 3374−3379.

(39) Forino, M.; Johnson, S.; Wong, T. Y.; Rozanov, D. V.; Savinov, A. Y.; Li, W.; Fattorusso, R.; Becattini, B.; Orry, A. J.; Jung, D.; Abagyan, R. A.; Smith, J. W.; Alibek, K.; Liddington, R. C.; Strongin, A. Y.; Pellecchia, M. Efficient synthetic inhibitors of anthrax lethal factor. *Proc. Natl. Acad. Sci. U.S.A.* **2005**, *102* (27), 9499−9504.

(40) Schepetkin, I. A.; Khlebnikov, A. I.; Kirpotina, L. N.; Quinn, M. T. Novel small molecule inhibitors of anthrax lethal factor identified by high-throughput screening. *J. Med. Chem.* **2006**, *49* (17), 5232−5244.

(41) Gualtieri, M.; Bastide, L.; Villain-Guillot, P.; Michaux-Characon, S.; Latouche, J.; Leonetti, J. P. In vitro activity of a new antibacterial rhodanine derivative against Staphylococcus epidermidis biofilms. *J. Antimicrob. Chemother.* **2006**, *58* (4), 778−783.

(42) Ma, Y.; Stern, R. J.; Scherman, M. S. Vissa, V. D.; Yan, W.; Jones, V. C.; Zhang, F.; Franzblau, S. G.; Lewis, W. H.; McNeil, M. R. Drug targeting Mycobacterium tuberculosis cell wall synthesis: Genetics of dTDP-rhamnose synthetic enzymes and development of a microtiter plate-based screen for inhibitors of conversion of dTDP-glucose to dTDP-rhamnose. *Antimicrob. Agents Chemother.* **2001**, *45* (5), 1407−1416.

(43) Dixon, M. The graphical determination of K_m and K_i. *Biochem. J.* **1972**, *129*, 197−202.

(44) Trager, W.; Jensen, J. B. Human malaria parasites in continuous culture. *Science* **1976**, *193*, 673−675.

(45) Lambros, C.; Vanderberg, J. Synchronization of *Plasmodium falciparum* erythrocytic stages in culture. *J. Parasitol.* **1979**, *65*, 418−420.

(46) Molecular Operating Environment (MOE 2001.07), Chemical Computing Group Inc., 1255, University St., Suite 1600, Montreal, Quebec, Canada, H3B 3X3.

(47) Goodsell, D. S.; Morris, G. M.; Olson, A. J. Automated docking of flexible ligands: Applications of AutoDock. *J. Mol. Recognit.* **1996**, *9*, 1−5.

(48) Morris, G. M.; Goodsell, D. S.; Huey, R.; Olson A. J. Distributed automated docking of flexible ligands to proteins: Parallel applications of AutoDock 2.4. *J. Comput.-Aided Mol. Des*. **1996**, *10* (4), 293−304.

(49) Mehler, E. L.; Solmajer, T. Electrostatic effects in proteins: Comparison of dielectric and charge models. *Protein Eng.* **1991**, *4* (8), 903−910.